Soft Nanoscience Letters, 2011, 1, 81-85
doi:10.4236/snl.2011.13015 Published Online July 2011 (http://www.scirp.org/journal/snl)

One-Step Preparation and Characterization of Zinc Phosphate Nanocrystals with Modified Surface

Jian Dong Wang[1], Da Li[1], Jin Ku Liu[1*], Xiao Hong Yang[2*], Jia Luo He[3], Yi Lu[1]

[1]Department of Chemistry, East China University of Science and Technology, Shanghai, China; [2]Department of Chemistry, Chizhou University, Anhui, China; [3]School of Materials and Engineering, Nanjing University of Technology, Nanjing, China.
Email: jkliu@ecust.edu.cn, yxh6110@yeah.net

Received February 14th, 2011; revised May 27th, 2011; accepted June 30th, 2011.

ABSTRACT

The surface-modified zinc phosphate ($Zn_3(PO_4)_2$) nanocrystals were synthesized by a facile and efficient one-step ultrasonic-template-microwave (UTM) assisted route. The crystal structure, optical properties and morphologies of zinc phosphate nanocrystals were characterized by X-ray diffraction, Fourier transform infrared spectroscopy, Raman spectroscopy and transmission electron microscope. And the TEM image showed that the product had good dispersion with a particle size of 30 - 35 *nm. The anti-corrosion function of anti-corrosive paint using zinc phosphate nanocrystals was researched and the experiment result showed that the salt atmosphere-resistant time was* 158 *h longer than that of zinc phosphate bulk materials on market. The performance of zinc phosphate nanocrystals with modified surface synthesized by one-step UTM assisted route was improved* 63.2% *compared with the bulk materials.*

***Keywords*:** *Synthesis, Ultrasonic, Microwave, Zinc Phosphate, Nanocrystals, Anti-Corrosion*

1. Introduction

Zinc phosphate, a non-toxic foundational material, has been widely applied in coating industry, medicine, electrical fields, especially anti-corrosion due to its low solubility in water/biological environment [1,2]. The crystal size has a great effect on the function of anti-corrosion due to the un-smoothness of the surface of metal basement. Meanwhile, the common technology of zinc phosphate production was hard to manufacture nanoscaled products. So, various techniques such as hydrothermal method [3-5], sol-gel method [6] and solid-state method [7] have been investigated for synthesis of zinc phosphate nanocrystals in the recent several years. However, these methods were difficult to be applied in the industry production because of the high cost and complicated technology. Especially, the dispersion of prepared zinc phosphate nanocrystals was very difficult in practical application. So, a method to prepare zinc phosphate nanocrystals with modified surface which is small enough with low-cost and simple way is the research object of many chemists.

The ultrasonic technology has been adapted to fabricate inorganic nanocrystals to improve the products' distribution [8,9]. And microwave-assisted synthesis was a new way to produce inorganic compounds because microwave heating is an in situ mode of energy conversion [10]. In this paper, the ultrasonic, microwave and triton x-100 were applied together in the synthesis of zinc phosphate nanocrystals for the first time and this method can be extended into the industry production for its low-cost and one-step reaction of preparations and surface modification. The product's anti-corrosion function was tested by the neutral salt spray (NSS) experiment and the result showed that the effective anti-corrosion time was obviously longer than that of the zinc phosphate bulk materials on market. This good performance was mainly owing to the small size and good-dispersion in painter. And the dosage of zinc phosphate nanocrystals would be reduced which could make the cost lower. The using of ultrasonic, microwave and triton x-100 in the synthesis process can decrease the crystal diameter and modify the surface. The triton x-100 shell covered on the surface of product can prevent the agglomeration of the products from the excess drying temperature in the drying process and improve the product' dispersion ability in the painter because of the dispersant effect of surfactant.

2. Experimental Section

2.1. Synthesis of Zinc Phosphate Nanocrystals

Into 0.1 mol/L $Na_3PO_4 \cdot 12H_2O$ solution of 20 mL and of 0.1 mol/L $Zn(NO_3)_2 \cdot 6H_2O$ solution of 30 mL in the clean beaker were added triton x-100 of 0.2 mL and 0.3 mL, respectively. The both reaction solutions were dropwise added into the 100 mL deionized water, and then the reaction system was put in the ultrasonic machine with continuous stirring until complete precipitate. And the reaction was carried out as the follow equation:

$$2Na_3PO_4 \cdot 12H_2O + 3Zn(NO_3)_2 \cdot 6H_2O \rightarrow Zn_3(PO_4)_2 \cdot 4H_2O + 6NaNO_3 + 38H_2O \quad (1)$$

Then, the white deposition was filtrated out, washed 3 times by deionized water and dried completely for 2 h in the microwave machine (The drying power was 400 W). Finally, after the product was dried completely, the zinc phosphate nanocrystals were obtained.

2.2. Characterization

The structures of the obtained products were characterized by X-ray powder diffraction (XRD, Shimadzu XD-3A diffractometer), Raman spectra (Jobin-Yvon) and Fourier transform infrared spectroscopy (IR, Nicolet Nagna-IR 550). The microstructures and morphologies were analyzed with transmission electron microscopy (TEM, Hitachi-800).

2.3. Experiment of Anti-Corrosion

The anti-corrosion function of the anticorrosive paint using zinc phosphate nanocrystals was tested by the neutral salt spray (NSS) experiment. [11] The 5 wt% NaCl aqueous solution was used as the corrodent and its pH should be kept between 6.5 and 7.2. The temperature of the test system was 35˚C and the sedimentation rate of salt fog was 2 mL/h (the incept area is 80 cm^2).

3. Results and Discussions

3.1. Morphologies and Structures

Figure 1(a) and **(b)** were the TEM images and selected area electron diffraction (SAED) image of zinc phosphate nanocrystals. **Figure 1(a)** clearly showed that the zinc phosphate nanocrystals had a uniform size with a diameter about 40 - 45 nm, good-dispersion and modified surface. The partial enlarged image of single zinc phosphate particle in **Figure 1(a)** expressed a core/shell structure with a zinc phosphate core of 30 - 35 nm and shell of about 5 nm. And the shell was the result of surface modified by triton x-100. The SAED image (**Figure 1(b)**) showed that the zinc phosphate nanocrystal was a polycrystal structure. In this study, the ultrasonic was used in the depositing process and it could enhance the vibration and shear between particles for its line-changed effect, which could promote the product separating better. [12] Microwave technology was applied in the drying process and it was also an effective way to avoiding agglomeration. Due to strong thermal gradients induced by microwave heating, strong stirring occurs for liquids leading to thermal uniformity of heated medium. [13,14] The triton x-100 was a surfactant in the precipitation which can reduce agglomeration and decrease the diameter of product. In the drying process, the triton x-100

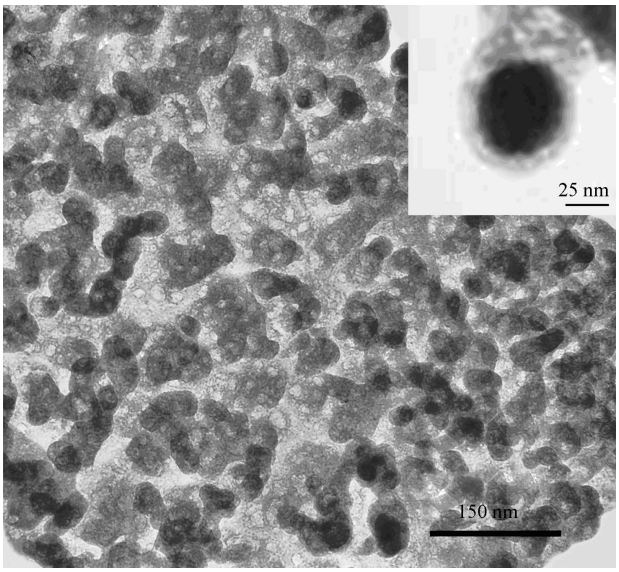

(a)

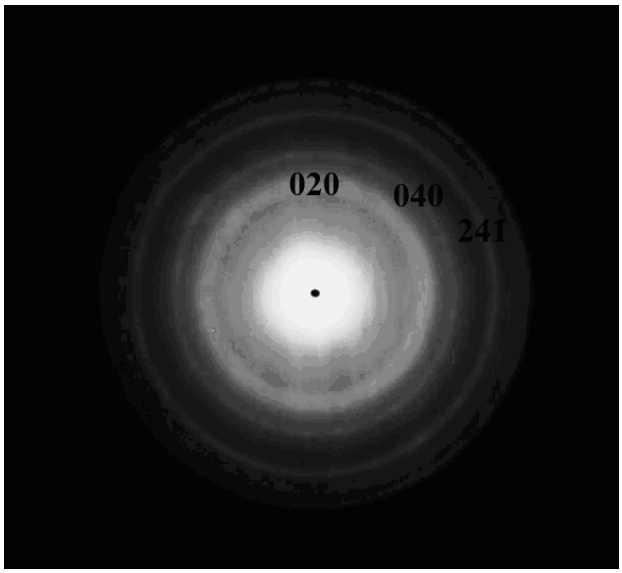

(b)

Figure 1. TEM images and SAED image of zinc phosphate nanocrystals.

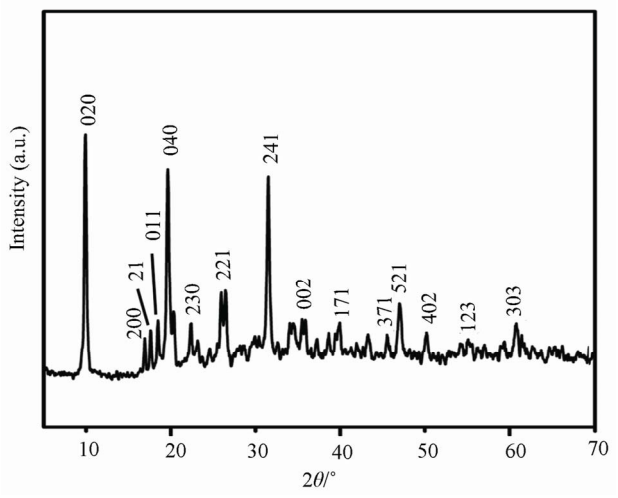

Figure 2. XRD pattern of zinc phosphate nanocrystals.

which can reduce agglomeration and decrease the diameter of product. In the drying process, the triton x-100 can prevent the possible integrality of crystal from over high temperature in the microwave heating machine. When the product was added into the resin to form the anti-corrosion painter, the zinc phosphate nanocrystals can disperse better than the ones without surface-modification because of the rule of similarity. From the **Figure 1(a)** and **(b)**, we can see that the UTM route can decrease the zinc phosphate's diameter and reduce the agglomeration effectively. Furthermore, the using of triton x-100 can improve the dispersion of zinc phosphate, prevent the agglomeration and modify the surface.

The XRD pattern of the zinc phosphate nanocrystals was shown in **Figure 2**. The fifteen strong peaks at 2-theta values of 9.65˚, 16.68˚, 17.79˚, 18.26˚, 19.38˚, 22.17˚, 25.67˚, 31.31˚, 35.67˚, 39.88˚, 46.78˚, 47.54˚, 49.94˚, 56.41˚ and 61.07˚ were thought to be originated from (020), (200), (210), (011), (040), (230), (221), (241), (002), (171), (371), (521), (402), (123) and (303) of crystal face of zinc phosphate ($Zn_3(PO_4)_2{\cdot}4H_2O$) which are matched with the standard XRD data of JC-PDS file (Numbers: 33-1474) [15].

According to Debye-Scherrer formula [16] estimates:

$$d = 0.89\lambda / \mathrm{B}\cos\theta \qquad (2)$$

The zinc phosphate particle size (core of modified products) of the products was about 34 nm which is consistent with the data in TEM images. When the ultrasonic, triton x-100 and microwave were used in the preparation, in the range of 2θ = 5˚ - 70˚, no other peaks could be observed which also confirmed that the product was exclusively $Zn_3(PO4)_2{\cdot}4H_2O$. In this research, the zinc phosphate nanocrystals without impurities can be prepared successfully by the UTM route.

3.2. Optical Properties

Figure 3(a) was the Raman spectrum for the zinc phosphate products. The absorption bands at 372 cm^{-1} and 870 cm^{-1} were attributed to P-O bending and stretching vibration, respectively. The absorption band within 1500 - 1750 cm^{-1} was the O-H stretching broad. The IR spectrum of zinc phosphate products were shown in **Figure 3(b)**. The O-H stretching broad band at 3378 cm^{-1} and 1640 cm^{-1} can be observed, implying the existence of crystal water. The several sharp absorption bands from 900 to 1200 cm^{-1} were a complex of stretching of PO_4^{3-} group as reported [17]. The absorption band at 1010 and 1120 cm^{-1} were the anti-symmetric stretching and symmetric stretching of PO_4^{3-}, respectively. The P-O bending vibration at 960 cm^{-1} was observed. The bending vi-

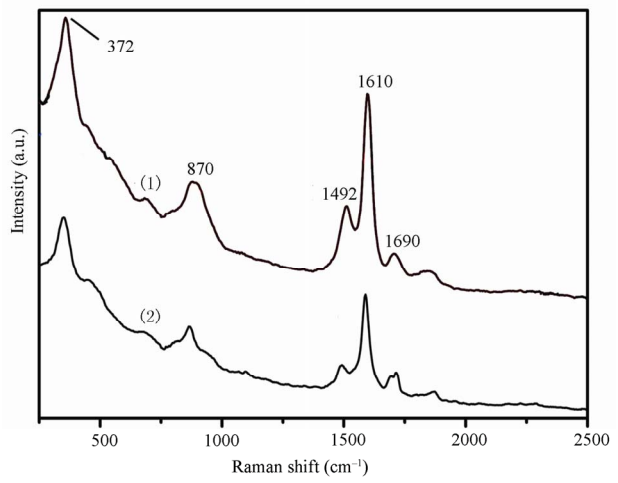

(a)

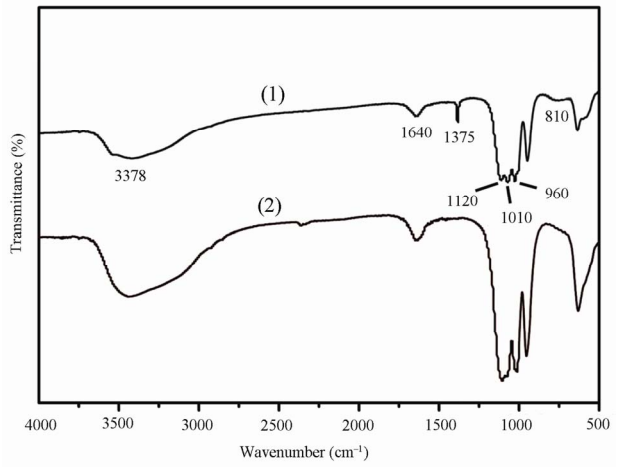

(b)

Figure 3. Raman (a) and IR spectrum (b) for zinc phosphate prepared by different ways: 1) nanocrystals; 2) bulk materials.

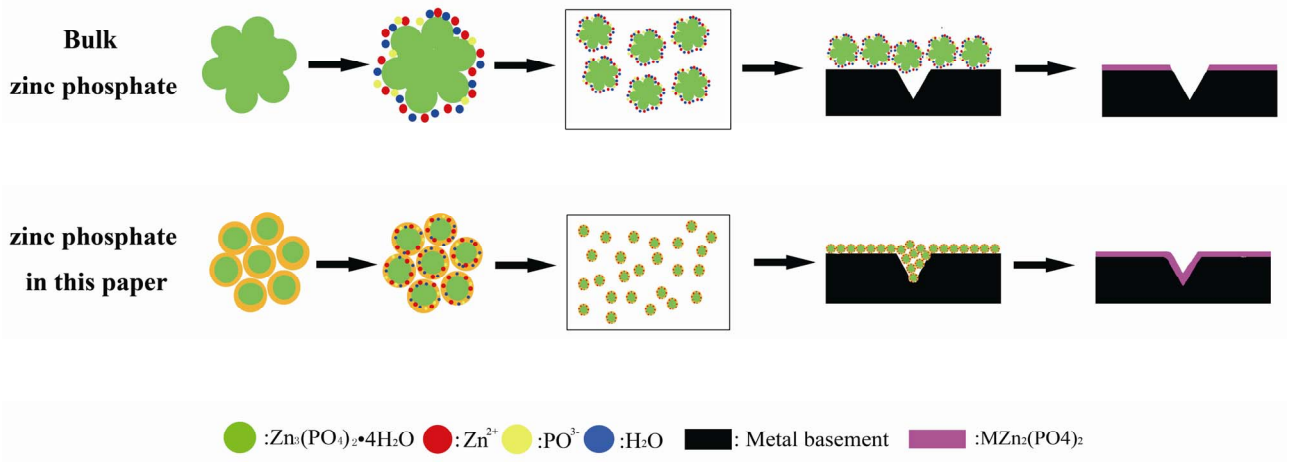

Figure 4. The anti-corrosion mechanism drawing of zinc phosphate.

bration at 960 cm^{-1} was observed. The bending vibration at 810 and 1375 cm^{-1} was the characteristic absorption peak of 1, 4-substituted phenyl and C-H symmetry bending vibration of methyl in triton x-100, respectively. These results showed that the zinc phosphate crystal was present, some crystal water existed in the product and the triton x-100 can be observed in the product synthesized by UTM route.

3.3. Anti-Corrosion Effect

The neutral salt spray experiment was going on to test the anti-corrosion function and salt spray was carried out for 1000 h and the sedimentation rate of salt fog was 2 mL/h (the incept area is 80 cm^2). The prohesion test was performed using 1150 cycles with 1 h spraying of 5 wt% NaCl aqueous solution at 35℃ and its pH should be kept between 6.5 and 7.2, followed by drying for 1 h. A paint horizontal scribe was used on the laboratory test specimens according to ISO/DIS standard 12944-6 [18]. For electrochemical measurements, two irony cells of 2.5 cm diameter and 3 cm high were used.

The result showed that effective anti-corrosion time was 408 h which was 158 h longer than zinc phosphate bulk materials on market. Because of the existence of crystal water inside the zinc phosphate crystal, a thin liquid layer formed in the surface of the product composed with Zn^{2+}, PO_4^{3-} and water. In the follow reaction equation, the M meant the composition of the metal basement.

$$Zn_3(PO_4)_2 + 6H_2O \rightarrow 2H_3PO_4 + 3Zn(OH)_2 \quad (3)$$

$$M + 2H_3PO_4 + 2Zn(OH)_2 \rightarrow MZn_2(PO_4)_2 + 4H_2O + H_2 \quad (4)$$

As the reaction (3) and (4) showed, the $Zn_3(PO_4)_2$ would hydrolyze into H_3PO_4 and $Zn(OH)_2$ due to the existence of the crystal water in the structure. Then, the H_3PO_4 and $Zn(OH)_2$ would react with the metal basement to form an undissolved complex of phosphate ($MZn_2(PO_4)_2$).When the zinc phosphate product had a touch with the metal basement, an undissolved complex of phosphate were produced to form a compact protective layer on the surface of the metal which can separate the metal basement from the corrosion. But in fact, the surface of metal basement was not smooth and intact, there were many indentations which can't be seen by eyes on it. According to the anti-corrosion mechanism drawing (**Figure 4**), it was hard for the zinc phosphate bulk material to touch inside the indentations and the metal was still corroded. In the other hand, the zinc phosphate nanosrystals can enter into the indentation and form a protective layer. Just because of this, the undissolved complex of phosphate formed by the zinc phosphate nanocrystals synthesized by the UTM route can avoid not only the electrochemical corrosion but also the chemical corrosion effectively.

4. Conclusions

In this paper, the surface-modified zinc phosphate nanocrystal was synthesized by UTM method in one step reaction and its dispersion were better than the ones which synthesized by the method reported before. The microwave and ultrasonic can not only prevent products reunion, but also improve the dispersion of product; the surface-modifying of triton x-100 can not only reduce the agglomeration of zinc phosphate nanocrystals in the reaction system and prevent the enlargement of the product's size from the excess drying temperature in the drying process, but also promote the dispersion of zinc phosphate in the painting. The NSS experiment was carried out and the result showed that the effective anti-corrosion time was 408 h which was obviously superior

to the 250 h of zinc phosphate bulk material on market; smaller size and better dispersion can enhance the anti-corrosion function of zinc phosphate nanocrystals and decrease the dosage of products. This method is eligible for the industry production because of its low cost and one-step reaction of preparation and surface modification.

5. Acknowledgements

This work was supported by the State Key Laboratory of Pollution Control, Resource Reuse Foundation (NO. PCRRF09005) and National Natural Science Foundation of China (21071024).

REFERENCES

[1] B. D. A. R. Romagnoli, V. F. Vetere and L. S. Hernandez, "Study of the Anticorrosive Properties of Zinc Phosphate in Vinyl Paints," *Progress in Organic Coatings*, Vol. 33, No. 1, 1998, pp. 28-35. doi:10.1016/S0300-9440(97)00124-0

[2] B. Czarnecka and J. W. Nicholson, "Ionrelease, Dissolution and Buffering by Zinc Phosphate Dental Coments," *Journal of Materials Science*: *Materials in Medicine*, Vol. 14, No. 7, 2003, pp. 601-604. doi:10.1023/A:1024018923186

[3] B. Yan and X. Z. Xiao, "Hydrothermal Synthesis, Controlled Microstructure, and Photoluminescence of hydrated $Zn_3(PO_4)_2$: Eu^{3+} Nanorods and Nanoparticles," *Journal of Nanoparticle Research*, Vol. 11, No. 8, 2009, pp. 2125-2135. doi:10.1007/s11051-008-9578-6

[4] B. Boonchom, R. Baitahe, S. Kongtaweelert and N. Vittayakorn, "Kinetics and Thermodynamics of Zinc Phosphate Hydrate Synthesized by a Simple Route in Aqueous and Acetone Media," *Industrial & Engineering Chemistry Research*, Vol. 49, No. 8, 2010, pp. 3571-3576. doi:10.1021/ie901626z

[5] O. Pawlig and R. Trettin, "Synthesis and Characterization of α -hopeite $Zn_3(PO_4)_2{\cdot}4H_2O$," *Materials Research Bulletin*, Vol. 34, No. 12, 1999, pp. 1959-1966. doi:10.1016/S0025-5408(99)00206-8

[6] B. I. Lee, W. D. Samuels, L. Q. Wang and G. J. Exarhos, "Sol-gel Synthesis of Phosphate Ceramic Composites," *Journal of Materials Research*, Vol. 13, No. 6, 1996, pp. 134-143. doi:10.1016/S0025-5408(99)00206-8

[7] Q. A. Yuan, S. Liao, Z. F. Tong, J. Wu and Z. Y. Huang, "Synthesis of Nanoparticle Zinc Phosphate Dihydrate by Solid State Reaction at Room Temperature and Its Thermochemical Study," *Materials Letters*, Vol. 60, No. 17-18, 2006, pp. 2110-2114.

[8] J. K. Liu, C. X. Luo, X. H. Yang and X. Y. Zhang, "Ultrasonic—Template Method Synthesis of CdS Hollow Nanoparticle Chains," *Materials Letters*, Vol. 63, No. 1, 2009, pp. 124-126. doi:10.1016/j.matlet.2008.09.029

[9] J. K. Liu, X. H. Yang and X. G. Tian, "Preparation of Silver/Hydroxyapatite Nanocomposite Spheres," *Powder Technology*, Vol. 184, No. 1, 2008, pp. 21-24. doi:10.1016/j.powtec.2007.07.034

[10] A. L. Jose and J. B. Kenneth, "Microwave Synthesis of NTHU-4 and Related Materials," *Microporous and Mesoporous Materials*, Vol. 113, No. 1, 2008, pp. 325-332.

[11] A. Amirudin and D. Thierry, "Corrosion Mechanisms of Phosphated Zinc Layers on Steel as Substrates for Automotive Coatings," *Progress in Organic Coatings*, Vol. 28, No. 1, 1996, pp. 59-76. doi:10.1016/0300-9440(95)00554-4

[12] F. L. Yuan, C. H. Chen, E. M. Kelder and J. Schoonman, "Preparation of Zirconia and Yttria-Stabilized Zirconia (YSZ) Fine Powders by Flame-Assisted Ultrasonic Spray Pyrolysis (FAUSP)," *Solid State Ionics*, Vol. 109, No. 1-2, 1998, pp. 119-123. doi:10.1016/S0167-2738(98)00108-8

[13] J. D. Wang, C. X. Luo, J. K. Liu and Y. Lu, "Synthesis of Yttria-Stabilized Cubic Zirconia Nanocrystals by Ultrasonic-Microwave Route," *NANO*, Vol. 5, No.5, 2010, pp. 271-277. doi:10.1142/S1793292010002177

[14] L. Combemale, G. Caboche, D. Stuerga and D. Chaumont, "Microwave Synthesis of Yttria Stabilized Zirconia," *Materials Research Bulletin*, Vol. 40, No. 3, pp. 529-536. doi:10.1016/j.materresbull.2004.10.024

[15] S. P. Yan, W. He and C. Y. Sun, "The Biomimetic Synthesis of Zinc Phosphate Nanoparticles," *Dyes and Pigments*, Vol. 80, No. 2, 2009, pp. 254-258. doi:10.1016/j.dyepig.2008.06.010

[16] J. C. Ray, R. K. Pati and P. Pramanik, "Chemical Synthesis and Structural Characterization of Nanocrystalline Powders of Pure Zirconia and Yttria Stabilized Zirconia," *Journal European Ceramic Society*, Vol. 20, No. 9, 2000, pp. 1289-1295. doi:10.1016/S0955-2219(99)00293-9

[17] M. Zhang, J. K. Liu, R. Miao, G. M. Li and Y. J. Du, "Preparation and Characterization of Fluorescence Probe from Assembly Hydroxyapatite Nanocomposite," *Nanoscale Research Letters*, Vol. 5, 2010, pp. 675-679. doi:10.1007/s11671-010-9530-4

[18] ISO/DIS 12944: Paint and Varnishes—Corrosion Protection of Steel Structures by Protective Paint Systems. Part 6—Laboratory Performance Test Methods, ISO, Geneva, 1998.

